

# Quark production in high energy electron positron collisions: from strange to top

Yuichi Okugawa,<sup>a,b,\*</sup> Adrian Irles,<sup>c,e</sup> Hitoshi Yamamoto,<sup>c,d</sup> François Richard<sup>a</sup> and Roman Pöschl<sup>a</sup>

<sup>a</sup>Université Paris Saclay,  
Orsay, France

<sup>b</sup>Tohoku University,  
Sendai, Japan

<sup>c</sup>Instituto de Física Corpuscular (IFIC),  
Paterna, Spain

<sup>d</sup>Universitat de Valencia,  
Paterna, Spain

<sup>e</sup>Consejo Superior de Investigaciones Científicas (CSIC),  
Paterna, Spain

E-mail: [yuichi.okugawa@cern.ch](mailto:yuichi.okugawa@cern.ch), [adrian.irles@ific.uv.es](mailto:adrian.irles@ific.uv.es),  
[yhitoshi@epx.phys.tohoku.ac.jp](mailto:yhitoshi@epx.phys.tohoku.ac.jp), [richard@lal.in2p3.fr](mailto:richard@lal.in2p3.fr),  
[poeschl@lal.in2p3.fr](mailto:poeschl@lal.in2p3.fr)

The process  $e^+e^- \rightarrow q\bar{q}$  with  $q\bar{q} = s\bar{s}, c\bar{c}, b\bar{b}, t\bar{t}$  plays a central role in the physics programs of high energy electron-positron colliders operating from  $O(100 \text{ GeV})$  to  $O(1 \text{ TeV})$  center of mass energies. Furthermore, polarized beams as available at the International Linear Collider (ILC) are an essential input for the complete measurement of the helicity amplitudes that govern the production cross section. Quarks, especially the heaviers, are likely messengers to new physics and at the same time they are ideal benchmark processes for detector optimization. All four processes call for superb primary and secondary vertex measurements, a high tracking efficiency to correctly measure the vertex charge and excellent hadron identification capabilities. Strange, charm and bottom production are already available below the  $t\bar{t}$  threshold. We will show with detailed detector simulations of the International Large Detector (ILD) that production rate and the forward backward asymmetries of the the different processes can be measured at the 0.1% to 0.7% level and how systematic errors can be controlled to reach this level of accuracy. The importance of operating at different center of mass energies and the discovery potential in terms of Randall-Sundrum models with warped extra dimensions will be outlined.

*International Conference on High Energy Physics*  
06-13 July 2022  
Bologna, Italy

\*On behalf of the ILD Concept Group

\*Speaker

## 1. Introduction

One of the physics observations that is anticipated at the future lepton colliders is the measurement of the vector and axial electroweak coupling between neutral vector bosons ( $Z^0$  and  $\gamma$ , potentially  $Z'$ ) and a quark pair through the  $e^+e^- \rightarrow q\bar{q}$  process. In the current Standard Model (SM), there is no definitive answer to explain the mass hierarchy of fermions. In fact, many models for the physics Beyond Standard Model (BSM), such as the Randall-Sundrum model [1], offers predictions of the aforementioned couplings in order to explain the hierarchy problem. Since the couplings between the Z boson and fermion pairs depends on the fermion helicities, it is also important to apprehend the initial and final states of the particles. The experimental approach for the measurements of coupling between the Z boson and  $q\bar{q}$  ( $q = c, b$ ) was first made by LEP and SLC collaborations through  $e^+e^- \rightarrow c\bar{c}$  and  $e^+e^- \rightarrow b\bar{b}$  at the Z-pole [2]. In the experiment, one can determine the couplings by measuring the the forward and backward asymmetry parameter ( $A_{FB}$ ) which is defined as:

$$A_{FB} = \frac{\sigma_F - \sigma_B}{\sigma_F + \sigma_B} \quad (1)$$

where  $\sigma_F$  ( $\sigma_B$ ) is the  $e^+e^- \rightarrow q\bar{q}$  cross section integrated over the forward (backward) hemisphere of the quark scattering angle  $\theta$ , with respect to the electron beam axis. These cross sections are determined from the polar angle of reconstructed track of  $q$  ( $\cos\theta_q$ ). Therefore, having a precise measurements in forward and backward cross section leads to the precision measurements of the couplings. In this analysis, the experimental methods and precision level of coupling measurements at the next generation lepton collider is introduced to demonstrate its capability and sensitivities towards new physics, using the full detector simulation of  $e^+e^- \rightarrow s\bar{s}$ ,  $c\bar{c}$ ,  $b\bar{b}$  and  $t\bar{t}$ .

## 2. ILC & ILD

The International Linear Collider (ILC) [3] is the electron-positron collider which is expected to run at  $\sqrt{s} = 250$  GeV at its launch. It is 20 km in length and can be extended to 30 km for  $\sqrt{s} = 500$  GeV. One of the key features of the ILC is the well defined initial and final states of the particles upon collision, since it can polarize both electron and positron beams. Such feature will enable the ILC to measure various physical observables to high precision, thus distinguishing theories on BSM (Fig.1). The International Large Detector (ILD) [5] is one of the detector complexes (along with SiD) that is proposed to be used at the running at the ILC. Its central trackers and highly granular calorimeters facilitates the high precision tracking and measurements for individual particles, which is achieved by the Particle Flow Algorithm, known as PFA [6]. PFA reconstructs Particle Flow Objects (PFO) of all the particle within an event, identifying individual charged and neutral particles, including the constituents inside the jets.

## 3. Event Reconstruction

The events are generated using WHIZARD 1.95 [7], along with parton shower simulation done by Pythia 6.422 [8]. The generated particles were then processed via full ILD GEANT4 detector simulation, which was used to produce the results shown here. A collision energy of  $\sqrt{s} = 250$  GeV

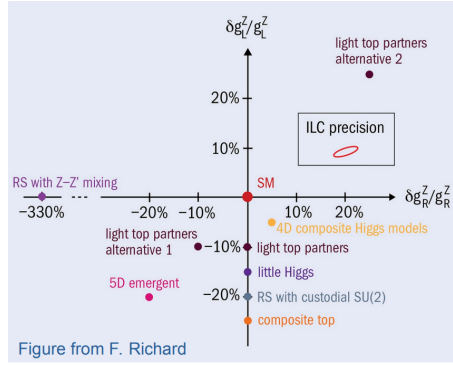


**Figure 1:** Predicted deviations of Z couplings to the left and right handed top quark [4]

53 was used for  $s\bar{s}$ ,  $c\bar{c}$ ,  $b\bar{b}$  production, and  $\sqrt{s} = 500$  GeV for  $t\bar{t}$  process. After the detector simulation  
 54 process, 2 jets were reconstructed using the Durham algorithm [9].

### 55 3.1 Flavor Tagging

56 Powerful flavor tagging techniques are essential to be able to separate the different channels we  
 57 are studying. Tagging of each jet requires precise measurement of impact parameter since such long  
 58 lived particles will decay at secondary vertices, the properties of which varies between different  
 59 flavors. In the Figure 2, the tagging efficiency and purity of  $b$  and  $c$  tags in ILD are shown as a  
 60 function of each flavor tagging cut. Their tagging performance show their resilience towards other  
 61 flavor backgrounds. After flavour tagging of the jets, the sum of the charges of PFOs associated  
 62 to each secondary vertex is used to form the vertex charge. For the  $b\bar{b}$  and  $t\bar{t}$  process, this is the  
 primary method to identify the generated quark charge, called *vertex method*.

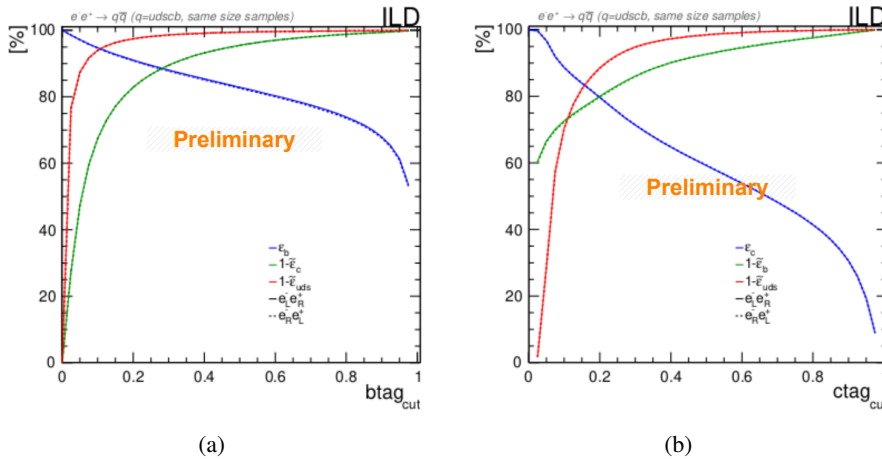


**Figure 2:** Flavor tagging performance for  $c$  (left) and  $b$  (right).  $\epsilon_c$  ( $\epsilon_b$ ) is the tagging efficiency after  $c$  ( $b$ ) tag cuts.  $1 - \tilde{\epsilon}_b$  ( $1 - \tilde{\epsilon}_c$ ) are the  $c$  ( $b$ ) tagging purity under  $b$  ( $c$ ) background.  $1 - \tilde{\epsilon}_{uds}$  is the flavor tagging efficiency under  $uds$  background. Finally, dotted and solid lines represent the same quantity with  $e_R^- e_L^+$  and  $e_L^- e_R^+$  beam polarization, respectively.

### 3.2 $dE/dx$ Measurements

Kaon identification can be the primary identifier for all flavors discussed in this analysis ( $s, c, b, t$ ) since they all could contain charged  $K$ :s at some point in their decay chain. Identification of charged  $K$ :s will give the information of the generated quarks, which is essential in calculating the  $A_{FB}$  for all  $e^+e^- \rightarrow q\bar{q}$  process here.  $dE/dx$  is the quantity of ionization energy loss within the differential distance and it is measured inside the Time Projection Chamber (TPC) of the ILD. For the particle identification,  $dE/dx$  distance is used with following definition:

$$dE/dx \text{ distance} = \text{signed} \left[ \left( \frac{(dE/dx - dE/dx_{exp-Bethe})}{\Delta_{dE/dx}} \right)^2 \right] \quad (2)$$

where  $dE/dx_{exp-Bethe}$  is  $dE/dx$  value expected from Bethe-Bloch formula,  $\Delta_{dE/dx}$  is the statistical error for  $dE/dx$  measurements, and the +/- sign that was lost upon squaring the quantity will be retained afterwards (thus "signed"). At the current working point, purity and efficiency for  $K$  identification using this method are 90 % and 80 %, respectively. Quark charge identification using  $dE/dx$  distance is called *Kaon method*.

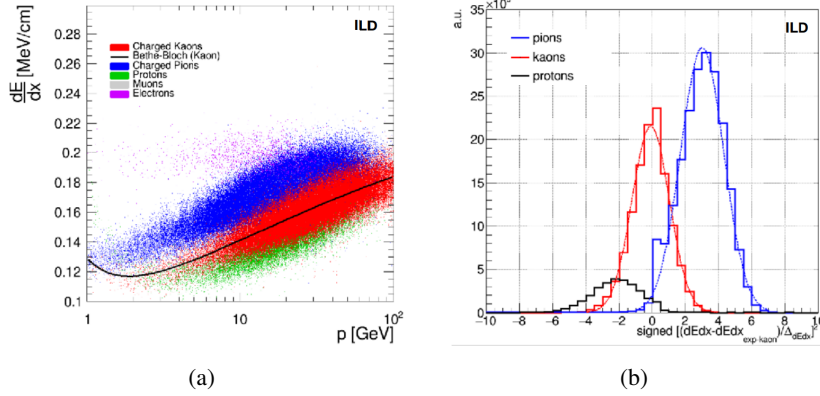


**Figure 3:** (a)  $dE/dx$  plotted against momentum for each particle ( $e, \mu, K^\pm, p, \pi$ ). (b)  $dE/dx$  distances from kaon Bethe-Bloch formula.

75

### 4. Asymmetry Measurements

As discussed in Section 1, particle charge measurement is the key to precisely measure  $A_{FB}$ . For this analysis, integrated luminosities of  $4,600 \text{ fb}^{-1}$  was taken for  $s\bar{s}$  process,  $900 \text{ fb}^{-1}$  for  $c\bar{c}$  and  $b\bar{b}$  process, and  $3,200 \text{ fb}^{-1}$  for  $t\bar{t}$  process. The polar angle distribution is the vital information for seeking the asymmetry parameter. In Figure 4, polar angle distribution for four different processes with beam polarization of  $e_L^- e_R^+$  are plotted with fit to the differential angular cross section:

$$\frac{d\sigma}{d \cos \theta} = S \times (1 + \cos^2 \theta) + A \times \cos \theta \quad (3)$$

where  $S$  and  $A$  are the symmetrical and asymmetrical parameter for the differential cross sections, respectively. Throughout four processes, all of their polar angle has good agreement with leading-order predictions, despite that  $s\bar{s}$ ,  $c\bar{c}$  and  $b\bar{b}$  has drop in the reconstruction efficiency above  $|\cos \theta| > 0.8$  due to the lack of acceptance of the detector at the forward region.

85

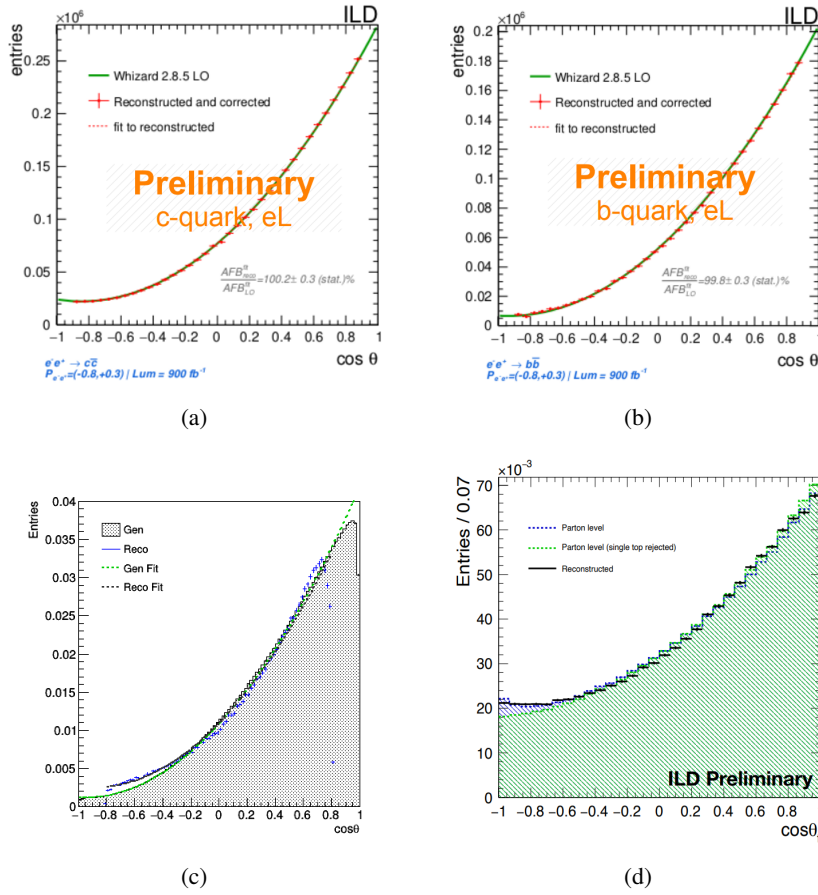


**Figure 4:** Polar angle distributions of 4 different processes plotted with generated  $q\bar{q}$  polar angle. (a)  $c\bar{c}$ , (b)  $b\bar{b}$ , (c)  $s\bar{s}$ , (d)  $t\bar{t}$

## 86 5. Systematic and Statistical Uncertainties

87 The  $A_{FB}$  measurements mostly suffers from the efficiencies of the charge identifications, as well  
 88 as the flavor tagging. In the Table 1, we show the results of systematic and statistical uncertainties  
 89 from  $c\bar{c}$  [10],  $b\bar{b}$  [11] and  $t\bar{t}$  [12] processes. The study of uncertainties for  $s\bar{s}$  process is still under  
 the investigation.

	stat. + syst.		stat.
	$c\bar{c}$	$b\bar{b}$	$t\bar{t}$
$\Delta A_{FB}(e_L^- e_R^+)$	$0.16\% + 0.09\%$	$0.15\% + 0.13\%$	$0.70\%$
$\Delta A_{FB}(e_R^- e_L^+)$	$0.20\% + 0.10\%$	$0.15\% + 0.095\%$	$0.53\%$

**Table 1:** Statistical and systematic uncertainties for three different processes with different beam polarization.

## 6. Conclusion

In this paper, the analysis methods for  $e^+e^- \rightarrow q\bar{q}$  at the ILC was demonstrated. Quark pair production with four different flavors ( $s\bar{s}$ ,  $c\bar{c}$ ,  $b\bar{b}$ ,  $t\bar{t}$ ) were generated with full detector simulation at the ILD. Vertex charge and  $dE/dx$  distance measurements were used to identify the quark charge and as a result, their reconstructed polar angle distribution showed great agreement with generated distribution. Moreover, flavor tag studies from  $c\bar{c}$  and  $b\bar{b}$  analysis demonstrated high performance in both efficiency and purity.

## References

- [1] L. Randall and R. Sundrum, *A Large mass hierarchy from a small extra dimension*, *Phys. Rev. Lett.* **83** (1999) 3370 [[hep-ph/9905221](#)].
- [2] ALEPH, DELPHI, L3, OPAL, SLD, LEP ELECTROWEAK WORKING GROUP, SLD ELECTROWEAK GROUP, SLD HEAVY FLAVOUR GROUP collaboration, *Precision electroweak measurements on the Z resonance*, *Phys. Rept.* **427** (2006) 257 [[hep-ex/0509008](#)].
- [3] T. Behnke et al., *The International Linear Collider Technical Design Report - Volume 1: Executive Summary*, [1306.6327](#).
- [4] F. Richard, *Present and future constraints on top EW couplings*, [1403.2893](#).
- [5] H. Abramowicz et al., *The International Linear Collider Technical Design Report - Volume 4: Detectors*, [1306.6329](#).
- [6] M. Thomson, *Particle flow calorimetry and the pandorapfa algorithm*, *Nuclear Instruments and Methods in Physics Research Section A: Accelerators, Spectrometers, Detectors and Associated Equipment* **611** (2009) 25.
- [7] W. Kilian, T. Ohl and J. Reuter, *WHIZARD: Simulating Multi-Particle Processes at LHC and ILC*, *Eur. Phys. J. C* **71** (2011) 1742 [[0708.4233](#)].
- [8] T. Sjöstrand, S. Ask, J. R. Christiansen, R. Corke, N. Desai, P. Ilten et al., *An introduction to PYTHIA 8.2*, *Comput. Phys. Commun.* **191** (2015) 159 [[1410.3012](#)].
- [9] S. Catani, Y. Dokshitzer, M. Olsson, G. Turnock and B. Webber, *New clustering algorithm for multijet cross sections in  $e^+e^-$  annihilation*, *Physics Letters B* **269** (1991) 432.
- [10] A. Irlles, R. Pöschl and F. Richard, *Production and measurement of  $e^+e^- \rightarrow c\bar{c}$  signatures at the 250 gev ilc*, 2020.
- [11] ILD collaboration, *Determination of the electroweak couplings of the 3rd generation of quarks at the ILC*, *PoS EPS-HEP2019* (2020) 624.
- [12] ILD CONCEPT GROUP collaboration, *International Large Detector: Interim Design Report*, [2003.01116](#).